



Published in final edited form as:

*J Clin Cell Immunol.* 2015 June ; 6(3): .

## Stable Expression and Characterization of an Optimized Mannose Receptor

David J Vigerust<sup>1,2,\*</sup>, Sherell Vick<sup>1</sup>, and Virginia L Shepherd<sup>1,2</sup>

<sup>1</sup>Department of Veterans Affairs Medical Center, USA

<sup>2</sup>Department of Pathology, Microbiology and Immunology, Vanderbilt University School of Medicine, Nashville TN 37212, USA

### Abstract

The mannose receptor (MR) is a macrophage surface receptor that recognizes pathogen associated molecular patterns (PAMPs) from a diverse array of bacterial, fungal and viral pathogens. Functional studies of the MR are hampered by the scarcity of human cell lines that express the receptor. Current model systems available for the study of MR biology often demonstrate low levels of expression and do not retain many of the classical MR properties. Although several laboratories have reported transient and stable expression of MR from plasmids, preliminary data from our laboratory suggests that these plasmids produce a protein that lacks critical domains and is often not stable over time. In this current report we describe the generation and characterization of a novel human codon-optimized system for transient and stable MR expression. Rare codons and sequences that contribute to mRNA instability were modified to produce mRNA that is qualitatively and quantitatively improved. Confocal imaging of the transient and stably expressed optimized receptor demonstrates a distribution consistent with previous reports. To demonstrate the functional characteristics of the optimized receptor, we further show that the introduction of codon-optimized MR plasmid can confer MR-associated phagocytosis of *S. aureus* to non-phagocytic HeLa cells. We show that three molecules participate in the engagement and internalization of *S. aureus*. MR was found to colocalize with Toll-like receptor 2 (TLR2) and Rab5 following exposure to pHrodo-stained *S. aureus*, suggesting cooperation among the three molecules to engage and internalize the bacterial particle. This study describes a transfection capable, optimized MR receptor with functional characteristics similar to the wild type receptor and further demonstrates a new system for the continued study of MR biology and function.

### Keywords

Macrophages; Mannose receptor

---

This is an open-access article distributed under the terms of the Creative Commons Attribution License, which permits unrestricted use, distribution, and reproduction in any medium, provided the original author and source are credited.

\*Correspondence author: Vigerust DJ, VA Medical Center/Research Service, 1310 24th Ave, South, Nashville, TN 37212, USA, Tel: 6158737352; Fax: 6158738561; Dvigerust@silverstaff.com.

## Introduction

The mannose receptor (MR) is a 175 kDa type I transmembrane protein and the prototype member of the C-type lectin family of proteins that includes the MR, Endo180, DEC205 and the phospholipase A2 receptor. The MR was initially described by Stahl and coworkers as a cell surface receptor on macrophages that is involved in the clearance of extracellular hydrolases [1], capture and clearance of pathogens [2], capture of foreign antigens for presentation to MHC-II compartments [3,4], clearance of glycoprotein hormones [5], clearance of extracellular peroxidases [6,7], endocytosis of lysosomal acid phosphatase [8], and regulation of glycoprotein homeostasis [9]. Structurally, the receptor contains a cysteine-rich domain, fibronectin type II repeat, and eight carbohydrate recognition domains (CRD), of which 4, 5 and 7 are reported to be invaluable to the binding and internalization of ligands with exposed oligosaccharides terminating in mannose, fucose or N-acetylglucosamine [10].

A defining feature of the MR is the capacity for rapid internalization from the plasma membrane via a clathrin-mediated mechanism that delivers the receptors and engaged cargo to the endocytic pathway [11,12]. Studies have shown that the MR engages ligands and mediates their internalization via receptor-mediated endocytosis [13,14], and participates in phagocytosis of mannosylated pathogens [15,16]. Ligands containing terminal sugars such as mannose bind at neutral pH to the MR at the cell surface and are brought into the cell. After dissociation in the acidic endosomal environment, ligands are delivered to the lysosomal compartment for degradation and the MR returns to the cell surface [17]. Reports suggest that 10–30% of the receptor at steady state resides on the cell surface and the remaining 70–90% is located in intracellular pools. The MR has a long half-life (>30 hours), and makes ten or more rounds of ligand internalization each hour [18].

In addition to their endocytic properties, several members of the MR family of molecules participate in phagocytosis, a function vital to the role of the macrophage in the innate immune response. Macrophages are present in virtually all tissues and are especially prominent in mucosal tissues. Within the context of innate immunity, macrophages are among the first cells to encounter an invading microorganism. The recognition capacity of the MR is broad and allows for the binding and uptake of a diverse array of pathogens including *Schistosoma mansoni* [19], *Paracoccidioides brasiliensis* [20,21] *Francisella tularensis* [22] *Candida albicans* [23], *Leishmania donovani* [24,25], *Mycobacterium tuberculosis* [26–28], *Pneumocystis jirovecii* [29], *Klebsiella pneumoniae* [30], HIV [31–33], Dengue virus [34], Hepatitis B [35], and influenza A [36,37]. Although mannose is not a common terminal carbohydrate residue on the cell surface of mammalian-derived proteins, it is commonly found on the surface of a variety of pathogens, thus allowing the MR to distinguish self from non-self through carbohydrate recognition.

The MR and MARCO (macrophage receptor with collagenous structure) have been identified as an opsonin-independent phagocytic receptor in the lung for *S. pneumonia* [38,39]. Dorrington et al. reported that MARCO is required for TLR2- mediated responses to *S. pneumoniae* [40] just as MR was reported to mediate internalization of *S. pneumoniae* in Schwann cells [41]. Additionally, recent investigation reveals that concentrations of

soluble MR are much higher in patients with pneumococcal bacteremia suggesting macrophage activation and placing MR as a new biomarker for invasive disease [42]. Mannose receptor and TLR2 are likewise involved in the recognition and response to *Paracoccidioides brasiliensis* [20,21]. During the course of particle internalization Rab5a and MR have been shown to cooperate. Mannose receptor levels and MR-mediated endocytosis are enhanced significantly in the presence of Rab5a [43]. Both endocytic and phagocytic events in the macrophage are activated by Rab5 [44]. The association of these molecules under endocytic and phagocytic conditions led to the hypothesis that these molecules would cooperate in bacterial clearance.

Few commonly used continuous macrophage cell lines express a functional MR, hampering studies on MR structure and function. Human THP-1 monocyte cells have been reported to express the MR following stimulation with phorbol myristate acetate (PMA) or phorbol ester 12-O-tetradecanoylphorbol-13-acetate (TPA) [45,46]. Diment et al. reported that MR expression could be induced on murine J774 cells following treatment with azacytidine, and our laboratory has described the characterization of the MR on the rat NR8383 macrophage line and the FDRC dendritic cell line [47,48]. Although these cell lines have provided model systems for MR studies, expression is often low and not all properties of the receptor are retained in these altered cells. Further complicating functional MR studies is the lack of an expression system that has been shown to result in production of a functional MR. Although several studies have reported transient and stable expression, preliminary work from our laboratory suggests that the MR protein that is produced lacks certain domains in the cytoplasmic tail, preventing accurate studies of trafficking and signaling mediated by the MR. A primary focus in our laboratory has been the study of the domains in the MR that mediate specific functions such as endocytosis and phagocytosis. To continue these studies, we have generated a codon-optimized MR cDNA that, when expressed, produces a full-length and functional MR. In the current report we describe the characterization of this codon-optimized MR cDNA and its stable expression in a continuous human cell line.

## Materials and Methods

### Codon optimization of the mannose receptor

Previous studies in our laboratory indicated that the wild type MR was difficult to express in mammalian cells and that the plasmid was unstable during long-term storage. Based on work from a number of laboratories indicating that specific sequences in mammalian genes contribute to difficulty in subsequent expression [49–51], we examined the MR sequence to determine codon bias, using the method of codon adaptation measurement described by Sharp and Li [52]. To identify single rare codons and rare codon clusters, online databases such as the Rare Codon Calculator (RaCC) were used. The MR gene optimized for mammalian codon usage with flanking *Bam*HI and *Eco*RI sites was synthesized by GeneArt (Regensburg, Germany) and cloned into a pcDNA 3.0 vector.

### Plasmids and antibodies

Anti-MR monoclonal antibody was obtained from BD Biosciences (San Jose CA), and anti-toll-like receptor (TLR)-2 and TLR-4 antibodies were obtained from Santa Cruz

Biotechnology (Santa Cruz, CA). Rab5 antibody was obtained from Cell Signaling Technology (Danvers, MA). Secondary antibodies conjugated to Alexa dyes 488, 555, and 647 for use in imaging studies were obtained from Invitrogen (Carlsbad CA). Phycoerythrin (PE)- or fluorescein isothiocyanate (FITC)-conjugated antibodies for use in fluorescent-activated cell sorting (FACS) were obtained from BD Biosciences (San Jose CA).

### Transfection of cells

Cells were transfected with FuGENE HD (Roche) transfection reagent according to the manufacturer's directions. Briefly, cells were cultured at a concentration of  $2 \times 10^6$  cells per P-100 dish overnight. Plasmid DNA (10  $\mu$ g) was incubated with transfection reagent and added to cells. The cells were incubated overnight at 5% CO<sub>2</sub> and 37° C. Following incubation, the cells were washed and DMEM (Gibco, Carlsbad CA) with 10% FBS and antibiotics was added. Cells were collected at 24 and 48 hours post-transfection for flow cytometry, imaging or immunoblot analysis. Cells were cultured in the presence of 1 mg/ml of G418 sulfate (Mediatech, Manassas VA) for selection of stable transfectants.

### Flow cytometry and confocal microscopy

Flow cytometry was performed using a FACSCaliber (BD Biosciences, San Jose CA) bench top analyzer in the Tennessee Valley Health System, Department of Veteran Affairs cytometry core facility. Cells were stained with FITC- or PE-conjugated anti-MR polyclonal antibodies as follows: cells were collected by centrifugation, followed by suspension in staining buffer (1% BSA, 0.1% sodium azide, 0.5% normal goat serum in PBS). Normal goat serum was included in the stain buffer to saturate Fc receptors and minimize non-specific fluorescence. The appropriate concentrations of FITC- or PE-conjugated antibodies were diluted in staining buffer and added to the cells. An isotype-matched control was also performed to account for non-specific fluorescence, and an unstained sample was included to account for auto fluorescence. The cells were incubated for 20 minutes in the dark at 4° C, and then washed twice with staining buffer followed by fixation in 500  $\mu$ l of 2% buffered paraformalin. The modulation of cell surface receptor density was represented as the percent change in mean fluorescence intensity as compared to the control. The number of events acquired for each sample was  $3 \times 10^4$  and cells were analyzed on a Becton Dickinson FACScan flow cytometer using CellQuest software or WinMDI FACS analysis software from J. Trotter (Scripps Research Institute, La Jolla CA).

Confocal microscopy was performed using a Zeiss LSM-510 confocal laser scanning inverted microscope in the Vanderbilt University imaging core facility. Cells were plated at a concentration of  $2 \times 10^5$  cells per 35 mm glass bottom Mattek tissue culture dish. Following treatment or incubation, cells were fixed in 2% buffered paraformalin followed by permeabilization with ice-cold methanol. Cells were then stained in a two-step process using mouse monoclonal anti-MR antibody followed by either goat anti-mouse Alexa-488 or Alexa-555 (Invitrogen, Carlsbad CA). The nucleus was stained for visualization with ToPro-3 (Invitrogen, Carlsbad CA). Cells were mounted in Aqua-polymount (Polysciences, Warrington PA) between coverslips. Images were collected at 520 nm using a 63 $\times$  or 100 $\times$  oil-immersion objective. Image processing was performed using Adobe Photoshop CS imaging software.

## Phagocytosis assay

Phagocytosis was assayed via uptake of pHrodo *S. aureus* BioParticles (Invitrogen, Eugene, OR). BioParticle conjugates are novel, no wash fluorogenic particles that are used for quantitative measurement of phagocytosis. Cells were cultured in complete media for 24 hours at a concentration of  $2 \times 10^5$  in Mattek tissue culture dishes. BioParticles prepared per manufacturer instructions were added to cells at a 5:1 ratio and cells plus particles incubated at 37°C for 30 minutes to allow for uptake. Cells were washed to remove unattached BioParticles, fixed in 2% paraformalin, stained with Alexa-488 conjugated anti-MR antibody, and prepared for confocal microscopy. Samples were examined by confocal microscopy using anti-MR Alexa-488, or Alexa 647-conjugated antibody against anti-TLR2 or Rab antibodies.

## Immunoblot analysis

Prior to transfection, cells were plated at a density of  $5 \times 10^5$  cells per well in 24-well plates or  $1 \times 10^6$  per P-100 tissue culture dish and incubated overnight in complete RPMI media. Following overnight incubation, fresh media was added and transfection or infection was performed. Following treatment, the cells were lysed in lysis buffer containing 0.5% NP-40. Total cellular protein was determined using the bicinchoninic acid (BCA) protein assay (Pierce, Rockford IL) and 10 µg of total protein was resolved by electrophoresis on a 7.5% SDS-PAGE gel at 150 volts constant at 40 C. Proteins were transferred to nitrocellulose at 100 volts followed by blocking in Licor Western blot block buffer. Immunoblot analysis was also performed on the Licor Odyssey platform using monoclonal anti-MR antibodies and goat anti-mouse IR dyes (Lincoln NE).

## Results

### Design of an MR cDNA for high-level expression in mammalian cells

Several recent studies have shown that rational design of mammalian genes can lead to higher level expression of heterologous genes [53]. For example, rare codons can dramatically limit mammalian protein expression in *E. coli*-based systems. The most commonly described codons include arginine (AGG, AGA, CGA), leucine (CTA), isoleucine (ATA), proline (CCC, and glycine (GGA). If these codons occur at a frequency higher than 1%, it is likely that translation will be negatively affected. In addition, clusters of these codons can reduce both the quantity and quality of synthesized protein [54,55]. The wild type human MR gene contains all of these codons, with significantly high levels of glycine and arginine rare codons, as well as doublet and triplet clusters as shown in Table 1. Data in Figure 1A shows the codon adaptation index (CAI) for the wild type and optimized MR sequence. In this measure, a value of 1 indicates the use of more common codons; any decrease in this number indicates more usage of rare codons. The CAI of 0.73 for the wild type MR correlates with the high percentage of rare codon usage as shown in Table 1, with the optimized MR sequence reaching almost 1. Data from a recent study suggested that wild type genes with a CAI of less than 0.78 were much less likely to properly express. As the CAI approached 1 through optimization, the genes demonstrated high levels of expression suggesting that the CAI was a strong measure of successful expression in mammalian cells [51]. The codon quality at each nucleotide position is shown in Figure 1B. In addition, other

studies have reported that low GC content as found in the MR (43%; Figure 1C) can lead to rapid mRNA turnover. Moreover, several negative cis-acting motifs were found which have been reported to hamper expression in mammals (Table 2; Figure 2A) [49,56–58].

Based on these observations, and the known difficulty in achieving high levels of transient and stable expression from plasmids expressing the wild type MR sequence, the gene was submitted to GeneArt for optimization to enhance mammalian expression. Analysis of the resulting cDNA sequence demonstrated that negative cis-acting sites had been avoided, including internal TATA-boxes, chi-sites and ribosomal entry sites, AT-rich and GC-rich sequence stretches, repeat sequences and RNA secondary structures, (cryptic) splice donor and acceptor sites, and branch points which may negatively influence expression [49,50,56]. Additionally, the GC-content was increased to 60% to prolong mRNA half-life (Figure 1C). Codon usage was further adapted to the preferred for Homo sapiens, resulting in a high codon adaption index value. The optimized gene was modified to contain a Kozac sequence to increase translational initiation and two STOP codons to ensure efficient termination. The final product was shown to have a maximum nucleotide identity of 75% compared to the wild type sequence archived in Genbank. The sequence was cloned into the pcDNA 3.0 mammalian expression vector for transient and stable transfection into human cells and designated optMR for these studies.

### **Transient expression of OptMR in 293T and HeLa cells**

Transient expression of optMR in HeLa cells demonstrated that the receptor protein was widely distributed within the cell with focal accumulations in the perinuclear region consistent with ER and Golgi localization (Figure 2B). The expression of optMR was robust and reproducible and is consistent with patterns of staining that are seen with primary macrophages and with the human hybridoma cell line 43MR [59].

### **Stable expression of OptMR in HeLa Cells**

The optMR plasmid was transfected into HeLa cells and stable transfectants were selected using G418. Flow cytometry was used to determine the presence and the quantity of MR on the surface of stable cells (Figure 3A), and intracellular localization was analyzed by confocal microscopy. Work from previous studies has reported that the MR is expressed on the surface of macrophages, with a significant portion localized in intracellular compartments including endosomes, phagosomes, and multivesicular bodies [12,43]. As shown in Figure 3B, the stably expressed receptor is uniformly distributed throughout the cytoplasm with small aggregates (Figure 3B), similar to transient expression (Figure 2B) and previous reports in primary macrophages [60]. Western blot analysis of HeLa cells expressing optMR showed that the protein expressed is approximately 175 kDa (data not shown) and is recognized by anti-MR antibody and produced as strong a signal as the MR found in macrophages and in the MR expressing human hybridoma cell line 43MR (Figure 3C) [59].

### **Engagement and phagocytic uptake of *Staphylococcus aureus***

A key function of the MR is the internalization of microorganisms through interaction of the receptor with exposed mannose groups on the foreign particle surface. We therefore



examined the ability of the expressed optMR to mediate phagocytosis of a particulate ligand. Stable transfectants were exposed to pHrodo-labeled *Staphylococcus aureus* (SA) for varying time periods ranging from ten minutes to several hours. Since the pHrodo-SA particle is sensitive to pH, only those particles that have been phagocytosed and localized to an intracellular acidic compartment will emit fluorescence. As shown in Figure 4E, as early as ten minutes post exposure, significant accumulations of the MR are seen at locations where the bacteria is located below the membrane. In several cases, the bacterial particle is encircled with MR in this particular focal plane. The brightfield image (Figure 4D) clearly shows that the particles are within the cell margins. These data suggest that the receptor is redistributed from a diffuse cytoplasmic localization to sites where challenge is present. Close analysis of the ring structure demonstrates that it is composed of several small accumulations or foci of MR. In many cases, the MR can clearly be seen to opsonize the particle.

### Receptor co-localization with Rab5 and TLR2

Further analysis suggests that the MR is participating with other cellular proteins to engage and internalize the SA particle. *S. aureus* has been previously described to be engaged by TLR2 and so we proceeded to determine if TLR2 was expressed in the MR stable HeLa cell line. The results of flow cytometry demonstrate that the relative levels of TLR2 on the cell surface of our stable cell line is comparable to the levels of MR expressed on the cell surface (Figure 3A) Staining of SA exposed HeLa OptMR with antibodies for toll-like receptor (TLR) 2 and 4 demonstrated that TLR2 but not TLR4 colocalized with MR. Results from these co-localization experiments demonstrated that MR and TLR4 did not co-localize together (data not shown) but TLR2 was found to traffic to the particle and encircle the SA (Figure 5A) along with the MR. Co-localization experiments were also performed with the Rab proteins 5 (Figure 5B) and 7. Rab5 and MR both likewise appear to traffic to and encircle the bacterial particle resulting in co-localization of the MR with TLR2 and Rab5. Infection of SA exposed cells did not result in the localization of TLR4 to the particle nor did TLR4 colocalize with MR. Rab 7 was also tested and did not colocalize with the MR or the SA particle.

### Discussion

The macrophage mannose receptor has been shown by a number of different laboratories to be a key receptor in the clearance of extracellular hydrolases and peroxidases, and to facilitate entry of numerous pathogens. Studies on the mechanisms underlying these processes including intracellular trafficking and interaction with potential cellular cofactors has been hampered by the difficulty in our laboratory and others to express a functional receptor from the mouse or human cDNA sequence [61]. Indeed, preliminary work from our laboratory suggests that expression of the MR from currently available cDNA plasmids results in a protein that lacks some key structural sequences and/or functions. We examined the MR gene to determine if specific sequences might be preventing high-level expression of MR protein. In the current study, we have developed an MR cDNA for optimal expression in mammalian cells based on eliminating rare codons, increasing G/C content, and removing other RNA structural features that might limit expression. The result is a stable MR cDNA

that can be expressed in *E. coli*, and can be transiently and stably expressed in human HeLa and 293T cells. The resulting MR protein expressed by HeLa and 293T cells has been structurally and functionally characterized, and appears to share many of the same features as the wild-type MR.

One of the first indications that the MR gene sequence itself might be hampering expression studies was the observation in our laboratory that the pcDNA3 vector itself was not stable upon storage, and could not be amplified in an *E. coli*-based system. In addition, any small amount of cDNA that could be isolated was not expressed to any measurable level in mammalian cells. Reports from other laboratories have suggested that selection of synonymous codons for a specific amino acid is not consistent among organisms, and may depend on a variety of factors including tRNA levels, G/C content, mutation frequency and patterns, and gene expression level [53]. Most often the codon usage presents problems when expression of heterologous genes is attempted, as in mammalian gene expression in *E. coli* or viral gene expression in mammalian cells. In our laboratory, we have previously encountered difficulties in expressing the MR cDNA in both *E. coli* systems as well as mammalian cells. Although little information is available concerning the effect of codon bias between different human cells and tissues, work from Plotkin and others suggest that codon usage could be tissue-specific [62]. One study of MR expression has been in the human macrophage cell line HL60. Results from this study suggest that control of cell surface expression of the MR may be tissue-and/or cell-specific [63].

In our current study we examined the expression of the MR using a cDNA optimized for high-level expression. The resulting cDNA, produced commercially by GeneArt, has lower rare codon usage, higher GC content, and reduced negative cis acting elements, all contributors to low protein expression (Tables 1 and 2; Figure 1). This approach has been used by a number of researchers to optimize expression of variety of plant and animal proteins, including a large study by Fath et al. where a direct comparison of 50 wild type and sequence optimized genes was performed [51]. High-level expression has resulted in enhanced ability to examine protein function in in vitro model systems. Optimization has also been applied clinically. In a recent study by Kosovac et al. sequence optimization was used to achieve high level and long-term expression of erythropoietin for enhanced gene delivery in vivo [64]. This report also showed high level expression correlated with higher GC content (CpG dinucleotides), consistent with the finding in the current study that increased GC content led to higher MR expression [64,65].

The wild type MR gene uses rare codons with a high frequency and contains a GC content that is quite low. These features affect expression by facilitating rapid mRNA turnover. Moreover, several negatively cis-acting motifs, which might hamper expression in mammals, were discovered. Following optimization of the gene, negative cis-acting sites (such as splice sites, poly (A) signals, etc.) were removed which may have previously negatively influenced protein expression (Table 1). GC-content was increased to prolong mRNA half-life (Figure 1C). Further, codon usage was adapted to the bias of *Homo sapiens* resulting in a high codon adaptation index value of 0.97 as compared to the wild type MR gene which had a codon adaptation index of 0.73 (Figures 1A and 1B). The parameter CAI (codon adaptation index) describes how well the codons match the codon usage preference



of the target organism. Thus, a CAI of 1.0 would be perfect [66]. However, a CAI of >0.9 is considered as very good (i.e. allowing high expression). The optimized gene therefore allows for high expression rates in HeLa cells (Figure 2). We determined that in transient conditions the receptor expresses efficiently and with a pattern of cellular distribution consistent with previous characterization of MR expression. The optimized MR protein was shown to be of the same molecular weight and was strongly recognized by anti-MR antibodies. The Western blot analysis demonstrated a protein of the same physical size and reactivity as the MR found in primary macrophages and in a previously described human hybridoma cell line that also expresses functional MR [59].

To determine if the codon-optimized MR can confer a phagocytic capacity, we have employed a pathogen of global concern and interest to illustrate the phagocytic properties of transfected cells. Serious infections from *Staphylococcus aureus* strains are increasing in recent years in populations at risk [67]. *S. aureus* is a normal human commensal and carriage species that typically results in infections of the skin and soft tissues [68]. Less frequently infections result in more serious outcomes, including sepsis, necrotizing fasciitis, osteomyelitis, and pneumonia [69]. MR stably expressed in HeLa cells was used to demonstrate that three molecules participate in the initial encounter between *S. aureus* and the healthy cell. MR co-localized with both TLR2 and Rab5 following exposure to pHrodo-stained *S. aureus*, suggesting cooperation among the three molecules to engage and internalize the bacterial particle. The cooperation of the MR with TLRs has recently been described for a variety of human pathogens such as *Pseudomonas aeruginosa* [70], *Paracoccidioides brasiliensis* [20], and *Mycobacterium tuberculosis* [28]. Cooperation has also been demonstrated after exposure to non-pathogenic bacteria [71] where it was shown that Gram positive bacteria activated the TLR2 pathway and the Gram negative bacteria activated the TLR4 pathway. Consistent with these findings we found that cooperation between MR and TLR2 following exposure to *S. aureus* but no cooperation was seen with TLR4. The interaction of MR with TLRs may prove to be very important in cases where secondary bacterial infection following virus infection as has been described. Bacterial-viral synergism contributing to serious disease has been described in HIV, influenza, dengue and respiratory syncytial virus [72–75]. Interestingly, these viruses also employ interaction with the MR as part of their entry and as a consequence alter the expression of MR on the surface of macrophages. The alteration of MR expression on the cell surface may prevent the appropriate recognition and clearance of bacteria providing an avenue for colonization and serious infection. The development of a receptor optimized for expression in a variety of cell types provides an important tool to better understand the sequences involved in microbial recognition, signalling and trafficking. We have established here a construct that biochemically, structurally and most importantly behaves exactly like the wild type MR found in macrophages.

## Acknowledgements

This work was supported by federal grants from the United States Department of Veterans Affairs (V.L.S, D.J.V). Confocal imaging and analysis were performed in part through the use of the Vanderbilt University Medical Center Cell Imaging Core Resource (Supported by NIH Grants CA68485, DK20593, and DK58404). Flow cytometry analysis was performed in the Tennessee Valley Health System, Department of Veterans Affairs flow cytometry facility.

## References

1. Stahl P, Schlesinger PH, Rodman JS, Doebber T. Recognition of lysosomal glycosidases in vivo inhibited by modified glycoproteins. *Nature*. 1976; 264:86–88. [PubMed: 1004542]
2. Pontow SE, Kery V, Stahl PD. Mannose receptor. *Int Rev Cytol*. 1992; 137B:221–244. [PubMed: 1478821]
3. Engering AJ, Cella M, Fluitsma D, Brockhaus M, Hoefsmit EC, et al. The mannose receptor functions as a high capacity and broad specificity antigen receptor in human dendritic cells. *European journal of immunology*. 1997; 27:2417–2425. [PubMed: 9341788]
4. Prigozy TI, Sieling PA, Clemens D, Stewart PL, Behar SM, et al. The mannose receptor delivers lipoglycan antigens to endosomes for presentation to T cells by CD1b molecules. *Immunity*. 1997; 6:187–197. [PubMed: 9047240]
5. Girod A, Storrie B, Simpson JC, Johannes L, Goud B, et al. Evidence for a COP-I-independent transport route from the Golgi complex to the endoplasmic reticulum. *Nat Cell Biol*. 1999; 1:423–430. [PubMed: 10559986]
6. Shepherd VL, Abdolrasulnia R, Garrett M, Cowan HB. Down-regulation of mannose receptor activity in macrophages after treatment with lipopolysaccharide and phorbol esters. *J Immunol*. 1990; 145:1530–1536. [PubMed: 2384669]
7. Lang T, Hellio R, Kaye PM, Antoine JC. Leishmania donovani-infected macrophages: characterization of the parasitophorous vacuole and potential role of this organelle in antigen presentation. *J cell sci*. 1994; 107:2137–2150. [PubMed: 7983173]
8. Imai K, Yoshimura T. Endocytosis of lysosomal acid phosphatase; involvement of mannose receptor and effect of lectins. *Biochem Mol Biol Int*. 1994; 33:1201–1206. [PubMed: 7804146]
9. Lee SJ, Evers S, Roeder D, Parlow AF, Risteli J, et al. Mannose receptor-mediated regulation of serum glycoprotein homeostasis. *Science*. 2002; 295:1898–1901. [PubMed: 11884756]
10. Taylor ME, Bezouska K, Drickamer K. Contribution to ligand binding by multiple carbohydrate-recognition domains in the macrophage mannose receptor. *The Journal of biological chemistry*. 1992; 267:1719–1726. [PubMed: 1730714]
11. Zvaritch E, Lambeau G, Lazdunski M. Endocytic properties of the M-type 180-kDa receptor for secretory phospholipases A2. *J Biol Chem*. 1996; 271:250–257. [PubMed: 8550569]
12. Harding C, Levy MA, Stahl P. Morphological analysis of ligand uptake and processing: the role of multivesicular endosomes and CURL in receptor-ligand processing. *Eur j of cell Biol*. 1985; 36:230–238. [PubMed: 2986980]
13. Stahl PD, Rodman JS, Miller MJ, Schlesinger PH. Evidence for receptor-mediated binding of glycoproteins, glycoconjugates, and lysosomal glycosidases by alveolar macrophages. *Proc Natl Acad Sci U S A*. 1978; 75:1399–1403. [PubMed: 274729]
14. Stahl P, Schlesinger PH, Sigardson E, Rodman JS, Lee YC. Receptor-mediated pinocytosis of mannose glycoconjugates by macrophages: characterization and evidence for receptor recycling. *Cell*. 1980; 19:207–215. [PubMed: 6766809]
15. Linehan SA, Martinez-Pomares L, da Silva RP, Gordon S. Endogenous ligands of carbohydrate recognition domains of the mannose receptor in murine macrophages, endothelial cells and secretory cells; potential relevance to inflammation and immunity. *Eur j immunol*. 2001; 31:1857–1866. [PubMed: 11433382]
16. Kang JX, Bell J, Leaf A, Beard RL, Chandraratna RA. Retinoic acid alters the intracellular trafficking of the mannose-6-phosphate/insulin-like growth factor II receptor and lysosomal enzymes. *Proc Natl Acad Sci U S A*. 1998; 95:13687–13691. [PubMed: 9811861]
17. Wileman T, Boshans R, Stahl P. Uptake and transport of mannosylated ligands by alveolar macrophages. Studies on ATP-dependent receptor-ligand dissociation. *The J Biol Chem*. 1985; 260:7387–7393. [PubMed: 3997876]
18. Wileman T, Boshans RL, Schlesinger P, Stahl P. Monensin inhibits recycling of macrophage mannose-glycoprotein receptors and ligand delivery to lysosomes. *Biochem J*. 1984; 220:665–675. [PubMed: 6087792]
19. Paveley RA, Aynsley SA, Turner JD, Bourke CD, Jenkins SJ. The Mannose Receptor (CD206) is an important pattern recognition receptor (PRR) in the detection of the infective stage of the

- helminth *Schistosoma mansoni* and modulates IFN $\gamma$  production. *Int j parasitol.* 2011; 41:1335–1345. [PubMed: 22036898]
20. Takahagi NE, Golim MA, Bannwart CF, Puccia R, Peracoli MT. Interactions between TLR2, TLR4, and mannose receptors with gp43 from *Paracoccidioides brasiliensis* induce cytokine production by human monocytes. *Med Mycol.* 2011; 49:694–703. [PubMed: 21417682]
  21. Balderramas HA, Penitenti M, Rodrigues DR, Bachiega TF, Fernandes RK, et al. Human neutrophils produce IL-12, IL-10, PGE2 and LTB4 in response to *Paracoccidioides brasiliensis*. Involvement of TLR2, mannose receptor and dectin-1. *Cytokine.* 2014; 67:36–43. [PubMed: 24680480]
  22. Schuler GS, Allen LA. Differential infection of mononuclear phagocytes by *Francisella tularensis*: role of the macrophage mannose receptor. *J leukoc Biol.* 2006; 80:563–571. [PubMed: 16816147]
  23. Porcaro I, Vidal M, Jouvert S, Stahl PD, Giaimis J. Mannose receptor contribution to *Candida albicans* phagocytosis by murine Eclone J774 macrophages. *J Leukoc Biol.* 2003; 74:206–215. [PubMed: 12885937]
  24. Chakraborty P, Ghosh D, Basu MK. Modulation of macrophage mannose receptor affects the uptake of virulent and avirulent *Leishmania donovani* promastigotes. *J Parasitol.* 2001; 87:1023–1027. [PubMed: 11695359]
  25. Akilov OE, Kasuboski RE, Carter CR, McDowell MA. The role of mannose receptor during experimental leishmaniasis. *J Leukoc Biol.* 2007; 81:1188–1196. [PubMed: 17261547]
  26. Li YJ, Petrofsky M, Bermudez LE. *Mycobacterium tuberculosis* uptake by recipient host macrophages is influenced by environmental conditions in the granuloma of the infectious individual and is associated with impaired production of interleukin-12 and tumor necrosis factor alpha. *Infection and immunity.* 2002; 70:6223–6230. [PubMed: 12379701]
  27. Schlesinger LS, Kaufman TM, Iyer S, Hull SR, Marchiando LK. Differences in mannose receptor-mediated uptake of lipoarabinomannan from virulent and attenuated strains of *Mycobacterium tuberculosis* by human macrophages. *J Immunol.* 1996; 157:4568–4575. [PubMed: 8906835]
  28. Kleinnijenhuis J, Oosting M, Joosten LA, Netea MG, Van Crevel R. Innate immune recognition of *Mycobacterium tuberculosis*. *Clin Dev Immunol.* 2011; 2011:405310. [PubMed: 21603213]
  29. Ezekowitz RA, Williams DJ, Koziel H, Armstrong MY, Warner A, et al. Uptake of *Pneumocystis carinii* mediated by the macrophage mannose receptor. *Nature.* 1991; 351:155–158. [PubMed: 1903183]
  30. Athamna A, Ofek I, Keisari Y, Markowitz S, Dutton GG, et al. Lectinophagocytosis of encapsulated *Klebsiella pneumoniae* mediated by surface lectins of guinea pig alveolar macrophages and human monocyte-derived macrophages. *Infection and immunity.* 1991; 59:1673–1682. [PubMed: 2019437]
  31. Liu Y, Liu H, Kim BO, Gattone VH, Li J, et al. CD4-independent infection of astrocytes by human immunodeficiency virus type 1: requirement for the human mannose receptor. *J Virol.* 2004; 78:4120–4133. [PubMed: 15047828]
  32. Nguyen DG, Hildreth JE. Involvement of macrophage mannose receptor in the binding and transmission of HIV by macrophages. *Eur J Immunol.* 2003; 33:483–493. [PubMed: 12645947]
  33. Debaisieux S, Lachambre S, Gross A, Mettling C, Besteiro S, et al. HIV-1 Tat inhibits phagocytosis by preventing the recruitment of Cdc42 to the phagocytic cup. *Nat Commun.* 2015; 6:6211. [PubMed: 25648615]
  34. Miller JL, de Wet BJ, Martinez-Pomares L, Radcliffe CM, Dwek RA, et al. The mannose receptor mediates dengue virus infection of macrophages. *PLoS Pathog.* 2008; 4:e17. [PubMed: 18266465]
  35. Op den Brouw ML, Binda RS, Geijtenbeek TB, Janssen HL, Woltman AM. The mannose receptor acts as hepatitis B virus surface antigen receptor mediating interaction with intrahepatic dendritic cells. *Virology.* 2009; 393:84–90. [PubMed: 19683778]
  36. Reading PC, Miller JL, Anders EM. Involvement of the mannose receptor in infection of macrophages by influenza virus. *J Virol.* 2000; 74:5190–5197. [PubMed: 10799594]
  37. Upham JP, Pickett D, Irimura T, Anders EM, Reading PC. Macrophage receptors for influenza A virus: role of the macrophage galactose-type lectin and mannose receptor in viral entry. *J Virol.* 2010; 84:3730–3737. [PubMed: 20106926]

38. Arredouani M, Yang Z, Ning Y, Qin G, Soininen R, et al. The scavenger receptor MARCO is required for lung defense against pneumococcal pneumonia and inhaled particles. *The Journal of experimental medicine*. 2004; 200:267–272. [PubMed: 15263032]
39. Arredouani MS, Yang Z, Imrich A, Ning Y, Qin G, et al. The macrophage scavenger receptor SR-AI/II and lung defense against pneumococci and particles. *Am J Respir Cell Mol Biol*. 2006; 35:474–478. [PubMed: 16675784]
40. Dorrington MG, Roche AM, Chauvin SE, Tu Z, Mossman KL, et al. MARCO is required for TLR2- and Nod2-mediated responses to *Streptococcus pneumoniae* and clearance of pneumococcal colonization in the murine nasopharynx. *Journal of immunology*. 2013; 190:250–258.
41. Macedo-Ramos H, Batista AF, Carrier-Ruiz A, Alves L, et al. Evidence of involvement of the mannose receptor in the internalization of *Streptococcus pneumoniae* by Schwann cells. *BMC microbiology*. 2014; 14:211. [PubMed: 25085553]
42. Rodgaard-Hansen S, Rafique A, Weis N, Wejse C, Nielsen H, et al. Increased concentrations of the soluble mannose receptor in serum from patients with pneumococcal bacteraemia, and prediction of survival. *Infectious diseases*. 2015; 47:203–208. [PubMed: 25650730]
43. Wainszelbaum MJ, Proctor BM, Pontow SE, Stahl PD, Barbieri MA. IL4/PGE2 induction of an enlarged early endosomal compartment in mouse macrophages is Rab5-dependent. *Exp Cell Res*. 2006; 312:2238–2251. [PubMed: 16650848]
44. Roberts RL, Barbieri MA, Ullrich J, Stahl PD. Dynamics of rab5 activation in endocytosis and phagocytosis. *J Leukoc Biol*. 2000; 68:627–632. [PubMed: 11073100]
45. Park EK, Jung HS, Yang HI, Yoo MC, Kim C, et al. Optimized THP-1 differentiation is required for the detection of responses to weak stimuli. *Inflammation research*. 2007; 56(1):45–50. [PubMed: 17334670]
46. Makino JI, Kamiya T, Hara H, Adachi T. TPA induces the expression of EC-SOD in human monocytic THP-1 cells: involvement of PKC, MEK/ERK and NOX-derived ROS. *Free Radic Res*. 2012; 46:637–644. [PubMed: 22313459]
47. Lane KB, Egan B, Vick S, Abdolrasulnia R, Shepherd VL. Characterization of a rat alveolar macrophage cell line that expresses a functional mannose receptor. *J Leukoc Biol*. 1998; 64:345–350. [PubMed: 9738661]
48. Harris N, Super M, Rits M, Chang G, Ezekowitz RA. Characterization of the murine macrophage mannose receptor: demonstration that the downregulation of receptor expression mediated by interferon-gamma occurs at the level of transcription. *Blood*. 1992; 80:2363–2373. [PubMed: 1421407]
49. Duan J, Antezana MA. Mammalian mutation pressure, synonymous codon choice, and mRNA degradation. *J Mol Evol*. 2003; 57:694–701. [PubMed: 14745538]
50. Espel E. The role of the AU-rich elements of mRNAs in controlling translation. *Semin Cell Dev Biol*. 2005; 16:59–67. [PubMed: 15659340]
51. Fath S, Bauer AP, Liss M, Spriestersbach A, Maertens B, et al. Multiparameter RNA and codon optimization: a standardized tool to assess and enhance autologous mammalian gene expression. *PLoS One*. 2011; 6:e17596. [PubMed: 21408612]
52. Sharp PM, Li WH. The codon Adaptation Index—a measure of directional synonymous codon usage bias, and its potential applications. *Nucleic Acids Res*. 1987; 15:1281–1295. [PubMed: 3547335]
53. Gustafsson C, Govindarajan S, Minshull J. Codon bias and heterologous protein expression. *Trends Biotechnol*. 2004; 22:346–353. [PubMed: 15245907]
54. Kane JF. Effects of rare codon clusters on high-level expression of heterologous proteins in *Escherichia coli*. *Curr Opin Biotechnol*. 1995; 6:494–500. [PubMed: 7579660]
55. Baca AM, Hol WG. Overcoming codon bias: a method for high-level overexpression of *Plasmodium* and other AT-rich parasite genes in *Escherichia coli*. *Int J Parasitol*. 2000; 30:113–118. [PubMed: 10704592]
56. Chen CY, Xu N, Shyu AB. mRNA decay mediated by two distinct AU-rich elements from c-fos and granulocyte-macrophage colony-stimulating factor transcripts: different deadenylation kinetics

- and uncoupling from translation. *Molecular and cellular biology*. 1995; 15:5777–5788. [PubMed: 7565731]
57. Fu, P. Introduction. In: Fu, P.; Panke, S., editors. *Systems Biology and Synthetic Biology*. Hoboken, NJ, USA: John Wiley & Sons, Inc.; 2009.
58. Chevalier-Mariette C, Henry I, Montfort L, Capgras S, Forlani S, et al. CpG content affects gene silencing in mice: evidence from novel transgenes. *Genome Biol*. 2003; 4:R53. [PubMed: 12952532]
59. Vigerust DJ, Vick S, Shepherd VL. Characterization of functional mannose receptor in a continuous hybridoma cell line. *BMC Immunol*. 2012; 13:51. [PubMed: 22967244]
60. Kang PB, Azad AK, Torrelles JB, Kaufman TM, Beharka A, et al. The human macrophage mannose receptor directs *Mycobacterium tuberculosis* lipoarabinomannan-mediated phagosome biogenesis. *J Exp Med*. 2005; 202:987–999. [PubMed: 16203868]
61. Le Cabec V, Emorine LJ, Toesca I, Cougoule C, Maridonneau-Parini I. The human macrophage mannose receptor is not a professional phagocytic receptor. *J Leukoc Biol*. 2005; 77:934–943. [PubMed: 15767290]
62. Plotkin JB, Robins H, Levine AJ. Tissue-specific codon usage and the expression of human genes. *Proceedings of the National Academy of Sciences of the United States of America*. 2004; 101:12588–12591. [PubMed: 15314228]
63. Pimpaneau V, Midoux P, Monsigny M, Roche AC. Characterization and isolation of an intracellular D-mannose-specific receptor from human promyelocytic HL60 cells. *Carbohydrate research*. 1991; 213:95–108. [PubMed: 1933956]
64. Kosovac D, Wild J, Ludwig C, Meissner S, Bauer AP, et al. Minimal doses of a sequence-optimized transgene mediate high-level and long-term EPO expression in vivo: challenging CpG-free gene design. *Gene Ther*. 2011; 18:189–198. [PubMed: 20944679]
65. Bauer AP, Leikam D, Krinner S, Notka F, Ludwig C, et al. The impact of intragenic CpG content on gene expression. *Nucleic Acids Res*. 2010; 38:3891–3908. [PubMed: 20203083]
66. Ramazzotti M, Brilli M, Fani R, Manao G, Degl'innocenti D. The CAI Analyser Package: inferring gene expressivity from raw genomic data. *In Silico Biol*. 2007; 7:507–526. [PubMed: 18391240]
67. Ray GT, Suaya JA, Baxter R. Trends and characteristics of culture-confirmed *Staphylococcus aureus* infections in a large U.S. integrated health care organization. *Journal of clinical microbiology*. 2012; 50:1950–1957. [PubMed: 22422853]
68. Landrum ML, Neumann C, Cook C, Chukwuma U, Ellis MW, et al. Epidemiology of *Staphylococcus aureus* blood and skin and soft tissue infections in the US military health system, 2005–2010. *JAMA : the journal of the American Medical Association*. 2012; 308:50–59. [PubMed: 22760291]
69. Aranha Camargo LF. Treatment of severe infections caused by *Staphylococcus aureus*: a change in the vancomycin paradigm? *Shock*. 2008; 30(Suppl 1):67–69. [PubMed: 18704006]
70. Xaplanteri P, Lagoumintzis G, Dimitracopoulos G, Paliogianni F. Synergistic regulation of *Pseudomonas aeruginosa*-induced cytokine production in human monocytes by mannose receptor and TLR2. *European journal of immunology*. 2009; 39:730–740. [PubMed: 19197942]
71. Dogi CA, Galdeano CM, Perdigón G. Gut immune stimulation by non pathogenic Gram(+) and Gram(-) bacteria. Comparison with a probiotic strain. *Cytokine*. 2008; 41:223–231. [PubMed: 18248820]
72. Igusa R, Sakakibara T, Shibahara T, Sakamoto K, Nishimura H, et al. Complicated secondary pneumonia after swine-origin influenza A virus infection in an immunocompetent patient. *The Tohoku journal of experimental medicine*. 2012; 226:117–120. [PubMed: 22251837]
73. Tsigrelis C, Mohammad M, Framow HS, Dellinger RP, Marchesani D, et al. Secondary bacterial pneumonia due to *Staphylococcus aureus* complicating 2009 influenza A (H1N1) viral infection. *Infection*. 2010; 38:237–239. [PubMed: 20237945]
74. Nagassar RP, Bridgelal-Nagassar RJ, McMorris N, Roye-Green KJ. *Staphylococcus aureus* pneumonia and dengue virus co-infection and review of implications of coinfection. *BMJ Case Rep* 2012. 2012
75. Groome MJ, Albrich WC, Wadula J, Khoosal M, Madhi SA. Community-onset *Staphylococcus aureus* bacteraemia in hospitalised African children: high incidence in HIV-infected children and

high prevalence of multidrug resistance. Paediatrics and international child health. 2012; 32:140–146. [PubMed: 22824661]

Author Manuscript

Author Manuscript

Author Manuscript

Author Manuscript



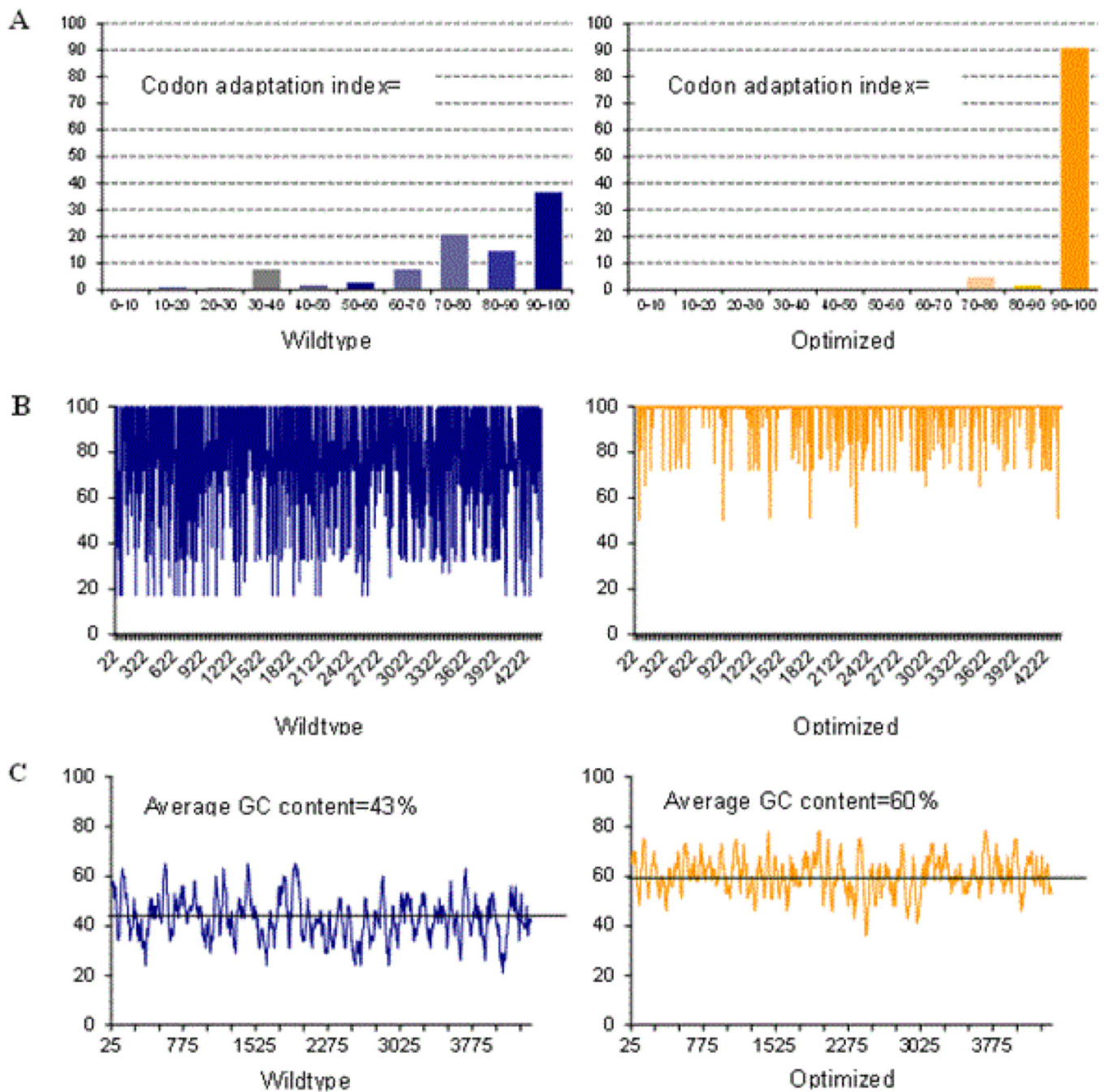


**Figure 1.**

Codon optimization of human MR. (A). The histograms show the percentage of sequence codons, which fall into a certain quality class. The quality value of the most often used codon for a given amino acid in the desired expression system is set to 100, the remaining codons are scaled accordingly [52]. (B). The plots show the quality of the used codon at the indicated codon position. (C). The plots show the GC content in a 40 bp window centered at the indicated nucleotide position.

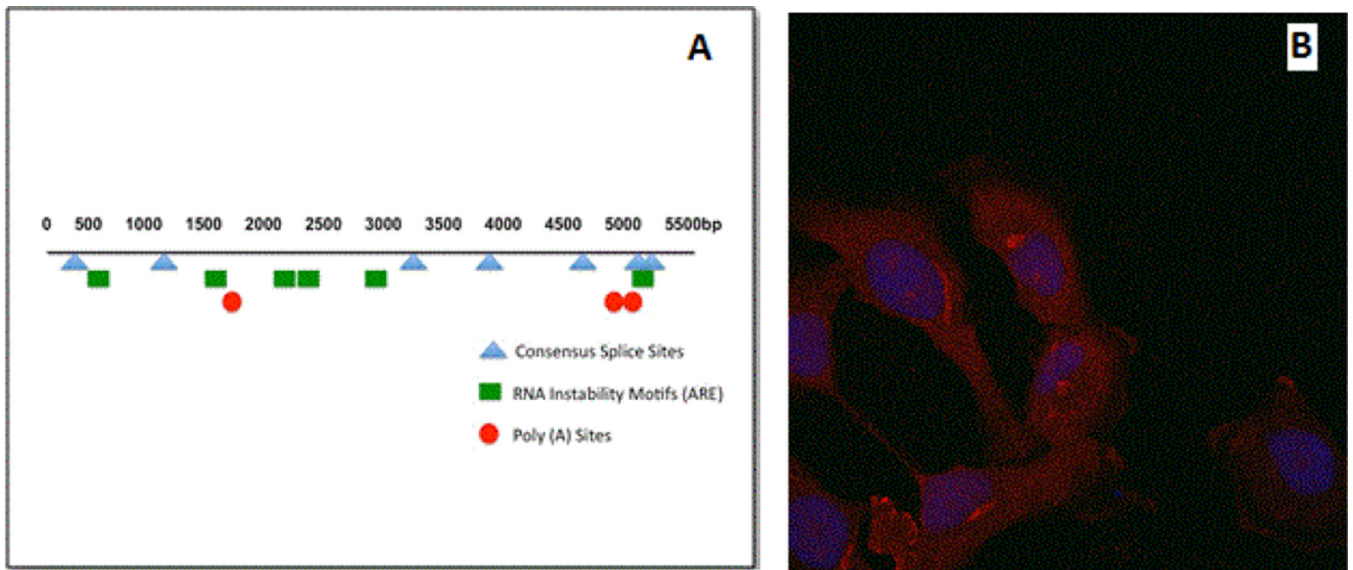
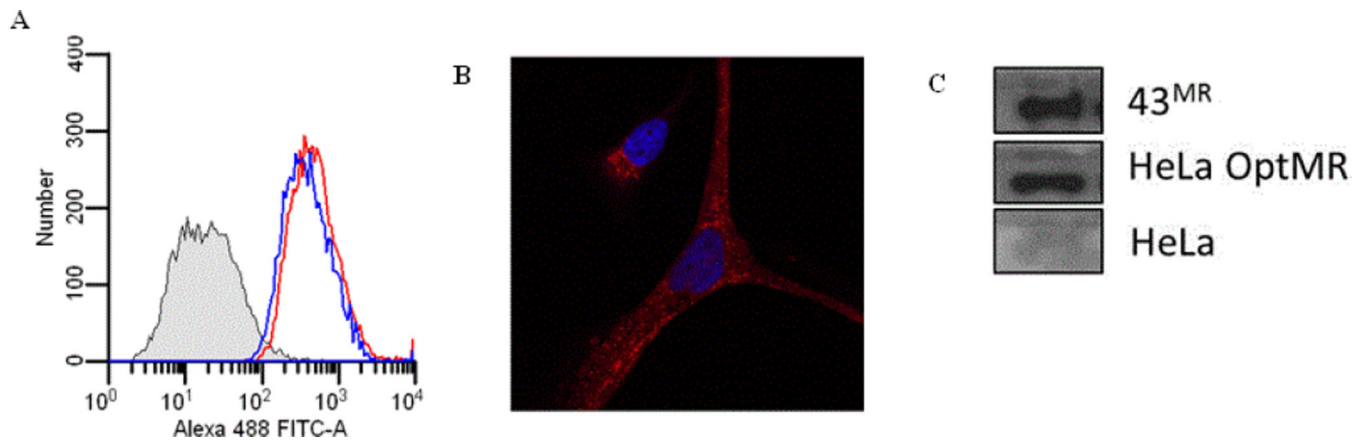


**Figure 2.**

Negative cis-acting motifs and transient transfectants. (A). Schematic representation of the relative positions within the MR gene where negative cis-acting motifs were removed. (B). Transient transfection of HeLa and 293T cells was performed with gene optimized MR. Following incubation, cells were stained with monoclonal anti-MR and secondary stained with goat anti-mouse Alexa 555. Nuclear staining is achieved with ToPro-3. Images were captured with a 63× oil objective on the Zeiss LSM-510 (B) Demonstrates the distribution of MR in HeLa cells transfected with OptMR after 48 hours incubation.



**Figures 3.**

Stable transfection of HeLa cells was performed with gene optimized MR. Stables were selected with 1 mg/ml of G418 sulfate. The cells were incubated under selection pressure for several weeks with change of media and addition of G418 sulfate every other day.

Following selection, cells were harvested and stained with monoclonal anti-MR and secondary stained with goat anti-mouse Alexa 488 or 555. Nuclear staining is achieved with ToPro-3. Images were captured with a 63× oil objective on the Zeiss LSM-510 (A)

Demonstrates the cytometric profile of MR and TLR2 in HeLa cells stably expressing OptMR after in 1mg/ml G418. Shaded histogram represents the unstained control, TLR2 expression in blue histogram and MR expression in the red histogram. (B) Demonstrates the distribution of MR within stable transfectants. (C) Western blot analysis was performed on cell lysate from stable transfectants.



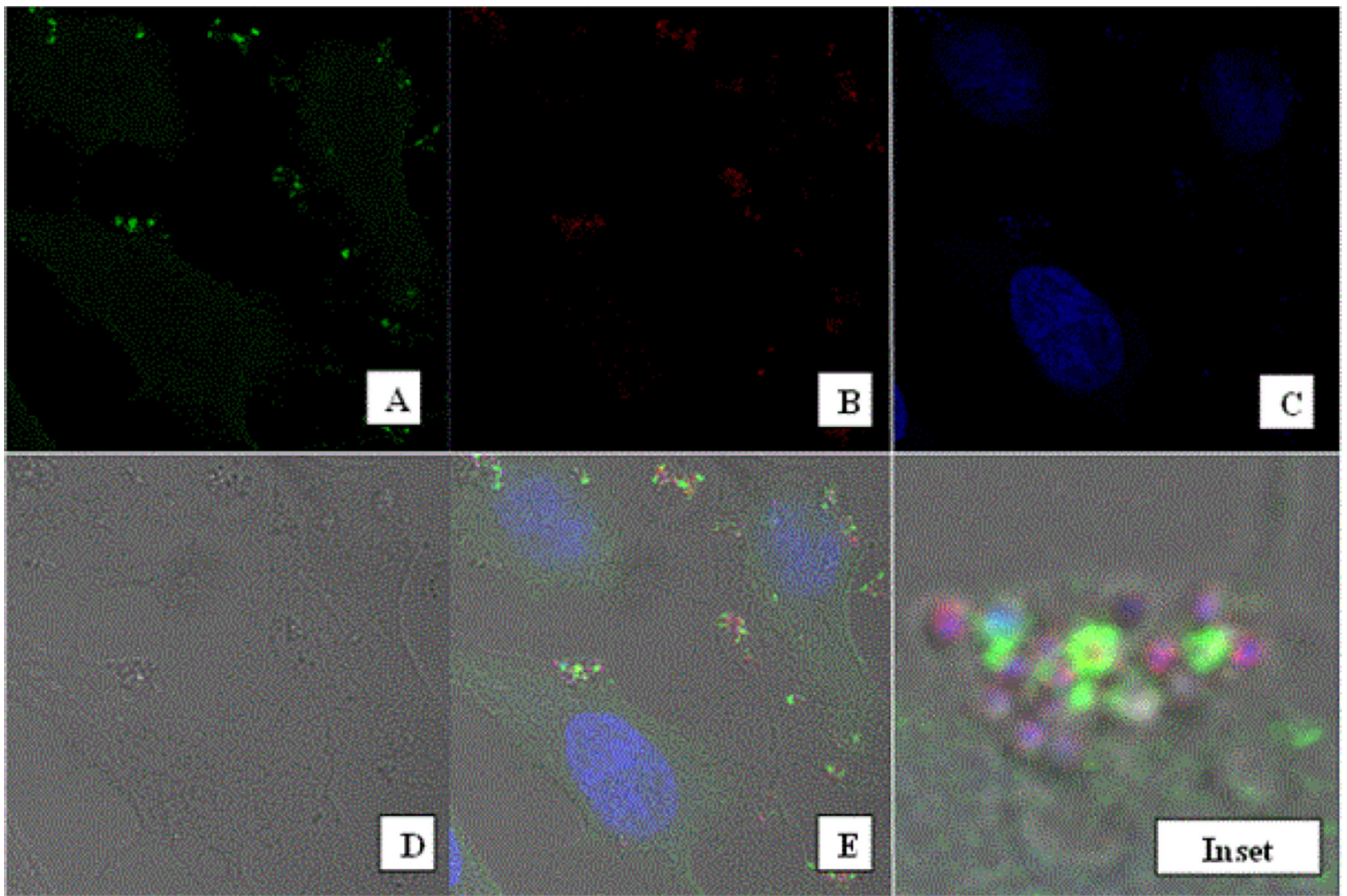


**Figure 4.** Phagocytosis of *Staphylococcus aureus* particles. HeLa OptMR stable transfectants were incubated with approximately 5:1 ratio of pHrodo SA particles per cell for 30 minutes. Following incubation, cells were stained with monoclonal anti-MR and secondary stained with goat anti-mouse Alexa 488. Images were captured with a 63 $\times$  oil objective on the Zeiss LSM-510 (A). pHrodo SA particles are shown (B). Nuclear staining was achieved with ToPro-3 (C). Brightfield view of the cells (D). Merge panel (E). Panel F shows the digital zoom of the designated inset in panel E.

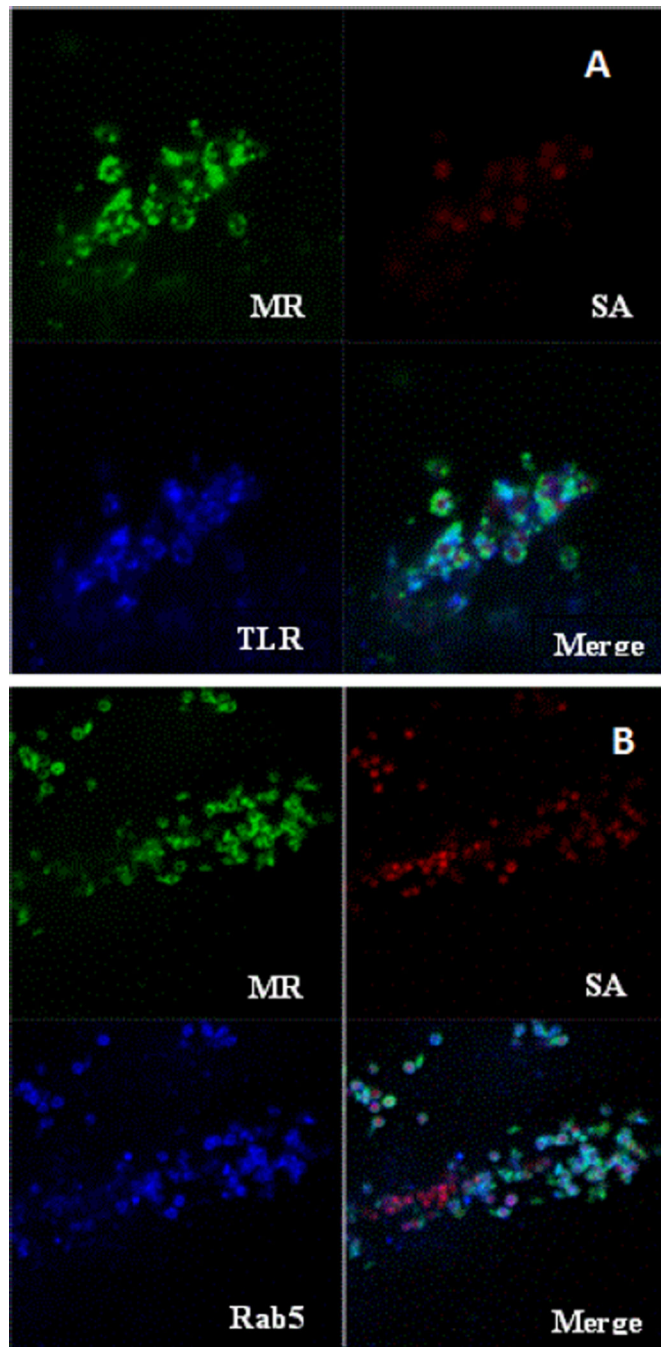


**Figure 5.**

Co-Localization of MR with cellular proteins TLR2 and Rab5. HeLa OptMR stable transfectants were incubated with approximately five pHrodo SA particles per cell for 30 minutes. Following incubation, cells were stained with monoclonal anti-MR and rabbit polyclonal anti-TLR2 (A) or Rab5a (B). Secondary staining with goat anti-mouse Alexa 488 and goat anti-rabbit 647. Images were captured with a 100× oil objective on the Zeiss LSM-510.

**Table 1**

Rare Codon Usage in the Wild type Mannose Receptor

Amino Acid/Rare Codons	#	%
Arginine: AGA, AGG, CGA	44	3
Glycine: GGA	39	2.7
Isoleucine: ATA	13	0.9
Proline: CCC	12	0.8
Leucine: CTA	11	0.8
Doublets	4	0.2
Triplets	3	0.2

Author Manuscript

Author Manuscript

Author Manuscript

Author Manuscript



**Table 2**

Comparison of wild type and optimized MR gene motifs

	Wild type MR	Optimized MR
<b>Prokaryotic inhibitory motifs</b>	12	0
<b>Poly (A) sites</b>	3	0
<b>Consensus (cryptic) splice donor sites</b>	4 (6)	0
<b>RNA instability motifs (ARE)</b>	8	0

Author Manuscript

Author Manuscript

Author Manuscript

Author Manuscript